Downloaded from orbit.dtu.dk on: Mar 15, 2025

DTU Library

Overview of the TWA concept from DEMO to the high power mock-up for WEST

Ragona, R.; Maquet, V.; Bader, A.; Batal, T.; Bernard, J.-M.; Chen, Z.; Courtois, X.; Delaplanche, J.-M.; Dumont, R.; Durand, F.

Total number of authors:
19

Published in:
AIP Conference Proceedings

Link to article, DOI:
10.1063/5.0163430

Publication date:
2023

Document Version
Publisher's PDF, also known as Version of record

Link back to DTU Orbit

Citation (APA):
Ragona, R., Maquet, V., Bader, A., Batal, T., Bernard, J.-M., Chen, Z., Courtois, X., Delaplanche, J.-M., Dumont, R., Durand, F., Durodié, F., Hillairet, J., Messiaen, A., Mollard, P., Nielsen, S. K., Ongena, J., Van Schoor, M., Xu, H., & Yang, Q. (2023). Overview of the TWA concept from DEMO to the high power mock-up for WEST. *AIP Conference Proceedings*, *2984*(1), Article 030014. https://doi.org/10.1063/5.0163430

General rights
Copyright and moral rights for the publications made accessible in the public portal are retained by the authors and/or other copyright owners and it is a condition of accessing publications that users recognise and abide by the legal requirements associated with these rights.

- Users may download and print one copy of any publication from the public portal for the purpose of private study or research.
- You may not further distribute the material or use it for any profit-making activity or commercial gain
- You may freely distribute the URL identifying the publication in the public portal

If you believe that this document breaches copyright please contact us providing details, and we will remove access to the work immediately and investigate your claim.

AIP Conference Proceedings

RESEARCH ARTICLE | AUGUST 18 2023

Overview of the TWA concept from DEMO to the high power mock-up for WEST FREE

R. Ragona ✉; V. Maquet; A. Bader; T. Batal; J.-M. Bernard; Z. Chen; X. Courtois; J.-M. Delaplanche; R. Dumont; F. Durand; F. Durodié; J. Hillairet; A. Messiaen; P. Mollard; S. K. Nielsen; J. Ongena; M. Van Schoor; H. Xu; Q. Yang

Check for updates

AIP Conference Proceedings 2984, 030014 (2023)
https://doi.org/10.1063/5.0163430

CrossMark

View Online

Export Citation

Articles You May Be Interested In

Progress on the design of a DEMO high power ICRH travelling wave antenna mock-up to be tested on WEST

AIP Conference Proceedings (September 2020)

Conceptual study of an ICRH traveling wave antenna (TWA) for T-15MD at 60 MHz

AIP Conference Proceedings (September 2020)

Study of the ohmic losses of a traveling wave antenna section in view of application on DEMO

AIP Conference Proceedings (September 2020)

22 August 2023 18:13:25

500 kHz or 8.5 GHz?
And all the ranges in between.
Lock-in Amplifiers for your periodic signal measurements

Find out more

Zurich Instruments

AIP Publishing

Overview of the TWA Concept from DEMO to the High Power Mock-up for WEST

R. Ragona,[1, a)] V. Maquet,[2] A. Bader,[3] T. Batal,[4] J-M. Bernard,[4] Z. Chen,[5] X. Courtois,[4] J-M. Delaplanche,[4] R. Dumont,[4] F. Durand,[4] F. Durodié,[2] J. Hillairet,[4] A. Messiaen,[2] P. Mollard,[4] S. K. Nielsen,[1] J. Ongena,[2] M. Van Schoor,[2] H. Xu,[5] and Q. Yang[5]

[1]*DTU, Technical University of Denmark, 2800 Kgs. Lyngby, Denmark*
[2]*Laboratory for Plasma Physics, Royal Military Academy, 1000 Bruxelles, Belgium*
[3]*ITER, Iter Organization, 13067 Saint Paul-lez-Durance Cedex, France*
[4]*CEA, IRFM, F-13108 Saint Paul-lez-Durance Cedex, France*
[5]*ASIPP, Institute of Plasma Physics, Chinese Academy of Science, 230031 Hefei Anhui, China*

[a)]Corresponding author: ricrag@fysik.dtu.dk

Abstract. The travelling wave array (TWA) concept was proposed as an RF actuator in the ion cyclotron range of frequencies (ICRF) for future fusion reactors and represents a relevant alternative to the conventional individually-fed arrays used in present-day machines. This paper presents an overview of the TWA concept, from the proposal for EU-DEMO to the successful tests of a high RF power mock-up paving the way for an experiment in a long-pulse device like WEST.
The best TWA integration case considered for a fusion reactor like EU-DEMO would be part of the breeding blanket, sharing its cooling and effectively acting as a first-wall component. The antenna should be insensitive to considerable mechanical deformations arising from the high-temperature operation of the blanket.
The roadmap to the proof-of-concept in a long-pulse device foresees a test at high power (up to 2 MW). We have designed and built a TWA antenna mock-up that has been successfully tested in the TITAN facility. This mock-up was an essential milestone that allowed us to demonstrate the validity of the design, confirming some key characteristics of the TWA concept. The ability to tune the antenna to be matched over a large frequency band was controlled in the design phase using trimmers and was well demonstrated during the experimental phase. The antenna frequency response showed to be resilient to thermo-mechanical deformations. The ohmic losses proved to be limited (4%). The expected operation targets were met (in TITAN) of 2 MW / 3 s and 500 kW / 60 s.
In the proof-of-concept, the antenna should minimize unwanted plasma-wall interactions (PWIs). The TWA already benefits from lower fields and a very narrow power spectrum due to the larger number of straps characterizing its structure. By adjusting the layout of the antenna, we show that the power spectrum can be tuned to avoid low-$|k_{\|}|$ excitation. Furthermore, we show that the electric fields on the antenna limiters can be reduced. The status, challenges and opportunities of the WEST TWA proof-of-concept proposal are discussed and future work is outlined.

22 August 2023 18:13:25

INTRODUCTION

A Travelling Wave Array (TWA) antenna consists of an array of mutually coupled elements supporting the propagation of a slow travelling wave [1] along its structure. It can be used in the Ion Cyclotron Range of Frequencies (ICRF) as an alternative to the phased arrays used in present-day tokamaks, and foreseen for ITER [2]. Ion Cyclotron Resonance Heating (ICRH) is a well-established technique foreseen to directly heat the ions in a fuel mix in the core of a large fusion machine [3]. ICRH can be used to heat high-density plasmas, as expected in a fusion reactor, where it does not suffer from high-density cut-offs. Additionally, ICRH could fulfil other tasks [4] as sawtooth pacing and impurity chasing during the ramp-up and landing phases, or burn control in the ignited phase. A drawback of ICRH is the challenge of coupling a large amount of power through an evanescent region in the plasma boundary [5], without producing undesirable effects like arcs on the antenna components or enhanced plasma-wall interactions (PWIs) giving rise to impurity that could contaminate the plasma core.

The TWA was initially proposed [6] for fast wave current drive (FWCD), due to its directional power spectrum and its load resilience property. The former is a consequence of a large number of radiating elements used. The latter is a consequence of the mutual coupling between elements determining the wave propagation [1, 6], with the plasma being only a small perturbation. This is in contrast to a conventional individually-fed phased array where the mutual coupling leads to unequal loading of the elements. A *slow wave* (transmission line) structure with elements closely resembling the current straps of present fast wave antennas is the *combline* [7, 8], which is a commonly used configuration for a commercially available bandpass filter. It is characterized by parallel elements that are short-

24th Topical Conference on Radio-frequency Power in Plasmas
AIP Conf. Proc. 2984, 030014-1–030014-10; https://doi.org/10.1063/5.0163430
Published by AIP Publishing. 978-0-7354-4604-5/$30.00

circuited at one end and open-circuited at the other end. Each element is a resonator, and each open end can be used as a tuning capacitance to tailor the frequency response of the structure.

A TWA is thus a multi-element array which requires only two feeding ports (input and output), as opposed to a phased array which requires independent feeding of each element. When operated within its bandpass, the structure presents a constant impedance to the feeding line. This impedance can be matched to the output impedance of the generator, maximizing its output power. In conventional antennas, this impedance matching is achieved by employing a matching circuit. When the number of elements increases, this matching circuit can become complex [9]. In a TWA, this matching is done intrinsically by the structure, resulting in a simpler system. Moreover, the voltages on the transmission lines and on elements like the vacuum feed-throughs are reduced for the same amount of injected power. This is due to the load, i.e., the antenna, being matched to the transmission line's characteristic impedance, giving a voltage standing wave ratio VSWR≈ 1. The capability of a TWA to maintain good impedance matching without dynamic tuning was experimentally demonstrated [10, 11], even during Edge Localized Modes (ELMs) [12, 13]. The TWA is thus a load resilient system. Moreover, this type of antenna presents additional advantages. The TWA power spectrum has a narrow toroidal extent. This high directivity enables localized power deposition into the plasma core [11, 14]. Additionally, the power spectrum was shown to be resilient to plasma loading variations [6]. The use of single-point feeding reduces the number of coaxial lines and feeders needed when compared to the individually fed straps of ICRF antennas used in most machines. This reduces the system's complexity and costs. The use of a larger number of straps reduces the power density of the antenna. Therefore, the voltage and currents on straps, and the maximum fields excited near the antenna, are reduced [15]. All the generator power can be delivered to the plasma by making the antenna long enough, such that no power reaches the output port, or this uncoupled power can be recirculated by means of a resonant ring [16, 17].

The TWA has been successfully tested on several devices to launch power in different heating regimes. For Fast Wave Current Drive (FWCD) [11, 18, 19], for Lower Hybrid (LH) [20, 21], and for Helicon waves excitation [22, 23, 24]. Additionally, it has been used for plasma production [11] and plasma start-up [21, 25]. More recently, the TWA concept was proposed as an ICRF launcher for the future fusion reactor EU-DEMO [4, 26], with a possible proof of concept in WEST [14]. The test on WEST is considered a technology demonstration for a TWA in a tokamak with a reactor-relevant metallic environment. Moreover, it could allow direct comparison with in-port ICRH antennas, under the same constraints.

22 August 2023 18:13:25

Similarly to other ICRF antenna concepts, the TWA should aim at minimizing the additional impurity influx induced during ICRF operations. Several physical phenomena like sheath rectification, ponderomotive force, and edge resonance, can concurrently take place during ICRF antenna operation. Current state-of-art models are not yet able to consider all those phenomena in the same simulations. However, guidelines for the antenna design have been created by gathering the experience of experimental campaigns and numerical modelling [27, 28]. The successful operation of an ICRH antenna with W limiters in ASDEX Upgrade (AUG) [28, 29] demonstrates the importance of decreasing the antenna near-fields, and consequently, the RF sheaths and related convective cells, arising from the RF image currents induced on the antenna structure and limiters. The minimization of the near-fields was also obtained in Alcator C-Mod, with an antenna aligned to the equilibrium magnetic field [30].
Additionally, the other field components around the antenna should also be minimized, as they can lead to other non-linear phenomena, e.g. a ponderomotive force [31]. Far-field effects could arise from antenna wave spectra exciting waves that are not well absorbed in the plasma core [32]. Recently, a good correlation was found between the low toroidal part of the antenna power spectrum and the generation of ICRF impurity in experiments minimizing the antenna near-fields [33]. The ideal antenna spectrum should maximize the power absorption in the plasma core with a reduced range of excited $k_{\parallel}$ wavenumbers, avoiding low-$|k_{\parallel}|$ spurious excitation [34, 35, 36].

The rest of the paper is organized as follows: In the next section, we review the TWA system proposed for EU-DEMO with particular emphasis on the integration aspects when considering an antenna embedded in the reactor breeding blanket. Subsequently, we present the TWA antenna proposed for WEST, summarizing the design activity carried out. Additionally, we summarize the results from the high-power mock-up experiments. In the following section, we focus on the plasma-wall interaction aspects and on the way to optimize the spectrum of the antenna to minimize those interactions. The most promising feeding system for a TWA is then presented, followed in the second to last section by a brief discussion on core physics aspects related to its use. Finally, the last section summarizes the paper and presents future possibilities.

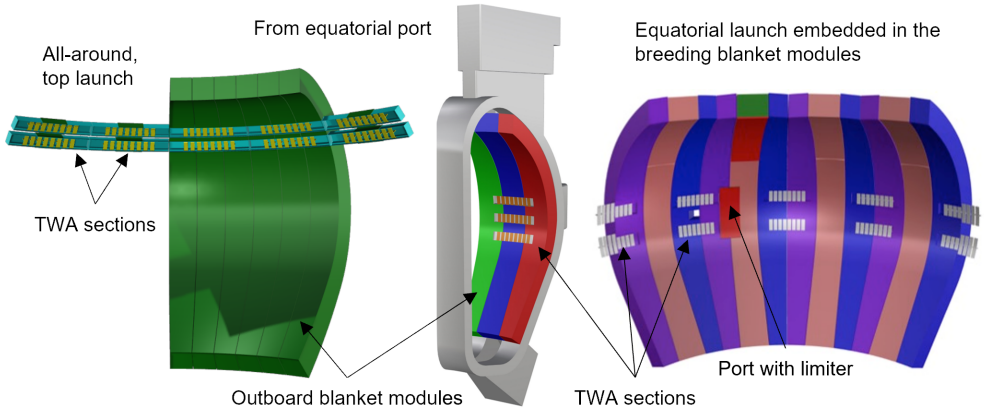

FIGURE 1. Different proposals of ICRF TWA antennas integrated into EU-DEMO. (left) a system based on arrays placed all around the device, fed from the top port. (center) TWA arrays are located in front of -and fed from- the equatorial port. (right) TWA arrays are periodically placed in every machine sector, fed from equatorial ports, and embedded in the breeding blanket.

A EU-DEMO TWA AND ITS INTEGRATION ASPECTS

During the years we have presented several configurations for an ICRF system based on the TWA concept as launcher [15, 26, 37], as an alternative to more classical phased arrays [38, 39]. The main requirement was the capability to deliver 50 MW of ICRF power, at low power density. Figure 1 shows three possible implementations with sections located all around the device, only in front of an equatorial port, or distributed in every sector around the equatorial plane. Initial studies explored a configuration with TWA sections placed in a ring all around the device, inserted in a recess of the breeding blanket modules. This system was able to couple the required power at low power density [40], mainly due to the large number of TWA sections employed (36, two for each machine sector), and the use of a resonant ring feeding scheme. The possibility to have a system based on a single-ring antenna instead of a sequence of separate sections was also considered [41]. However, this configuration was discarded due to coupling issues between generators. Feeding all straps individually was also discarded due to the large number of feeding lines required.
The system based on sections scattered all around the device, at a high poloidal location with access from the top port of the device was proposed in [37]. It was characterized by a power density of ≈ 1 MW/m^2 and a maximum voltage on the straps of 15 kV, when loaded with a reference plasma profile. The possibility of having the antenna sections located only close to a reduced number of equatorial ports (Fig. 1,center) was explored in [26]. The reduced number of elements increased the power density to ≈ 3 MW/m^2 and the maximum voltage to 30 kV.
Finally, a configuration with elements scattered symmetrically in the equatorial plane in every section of the device (Fig. 1,right) was presented in [42]. The power density of this design was ≈ 1.1 MW/m^2.

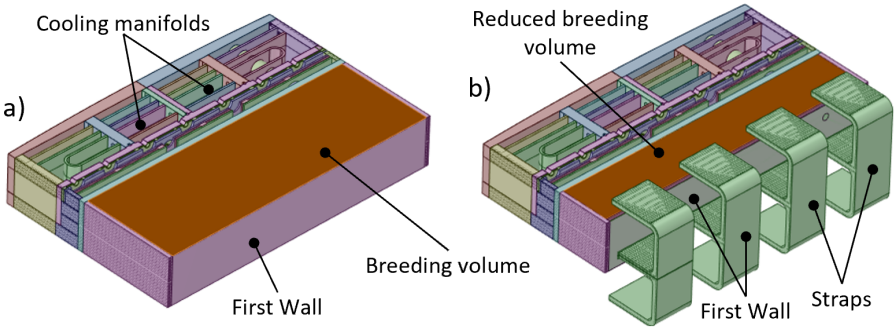

FIGURE 2. (a) Breeding Blanket section showing the cooling manifolds, the neutron multiplier, and the first wall components. This is for an unmodified section. (b) Modified section of the breeding blanket where a part of the neutron multiplier was reduced to give space to the straps of the TWA antenna.

22 August 2023 18:13:25

An initial integration study was carried out in [37] using, as a reference blanket, the Helium Cooled Pebble Bed (HCPB) breeding blanket design [43]. This blanket design is characterized by the presence of radial *fuel-breeder pins* which gives a series of benefits when compared to poloidally running pins. In particular, they provide more "*flexibility to allocate penetrating systems (e.g. equatorial ports)*" [43], or like a distributed TWA antenna. Figure 2a shows an equatorial slice of a HCPB blanket module, with the cooling manifolds, the breeding zone and the first wall (FW) highlighted. The integration of a TWA works as follows. The breeding zone is reduced in depth and the straps are connected to the FW. The pins are used to support the straps and to provide cooling, sharing the same cooling circuit of the breeding blanket. The straps are part of the FW, and are built with the same functionality. Material constraints do not allow the use of low-loss materials usually used in RF antennas, like copper or silver. Therefore, the chosen material is Eurofer covered with tungsten. Figure 2b shows the blanket slice with reduced depth and with the strap integrated. Thermo-mechanical analyses of the actively-cooled strap structure provide the order of magnitude of the deformations expected in a reactor scenario. This information was incorporated in the design of the mock-up for the technology demonstrator on WEST, discussed in the next section. An extensive analysis of the integration in the HCPB blanket was recently carried out and it will be published in a future paper [44]. Moreover, a neutron transport code (MCNP) was used to evaluate the impact on the tritium breeding ratio (TBR). The reduction of TBR is within 2% for a series of antenna sections placed all around the device, occupying almost 6% of the blanket volume. This is explained by the fact that the breeding volume of the blanket is reduced in depth by a few centimetres, while keeping its functionality. The work took into account a realistic and detailed description of the TWA elements. The feeding lines could be routed in place of a radial pin, and were considered in the MCNP calculations. The definition of the interface between the straps and the feeding lines is the subject of future work.

TWA TECHNOLOGY DEMONSTRATOR ON WEST

For EU-DEMO, we proposed to demonstrate the technology of a reactor-relevant ICRF system based on the TWA concept with a TWA system for WEST. Figure 3 shows the most recent version of the TWA antenna integration proposed for WEST. A description of the system and of its performance, when compared to a WEST antenna, were presented in [14]. The system was based on two TWA sections, fed by two resonant rings. A detailed description of this feeding scheme is given in a subsequent dedicated section The antenna was designed to replace one of the installed WEST ICRH antennas. The nominal design performances are 3 MW for 30 s and 1 MW for 1000 s. The WEST TWA antenna mock-up mechanical design and thermal-structural analysis were presented in [45] while the RF design was described in [46]. The antenna was designed as an array with 6 elements. The capacitors to tune the antenna are formed by the metallic surfaces of the straps enclosed in metallic cavities. The capacitor layout was made symmetric and tailored to demonstrate the possibility of realizing a large bandwidth (BW) of 10 MHz, representing a fractional BW of $\approx 20\%$. Special trimmers were designed for the capacitors allowing corrections or modifications of the antenna response. One WEST generator was connected to the TWA input, and the output to a dummy load.

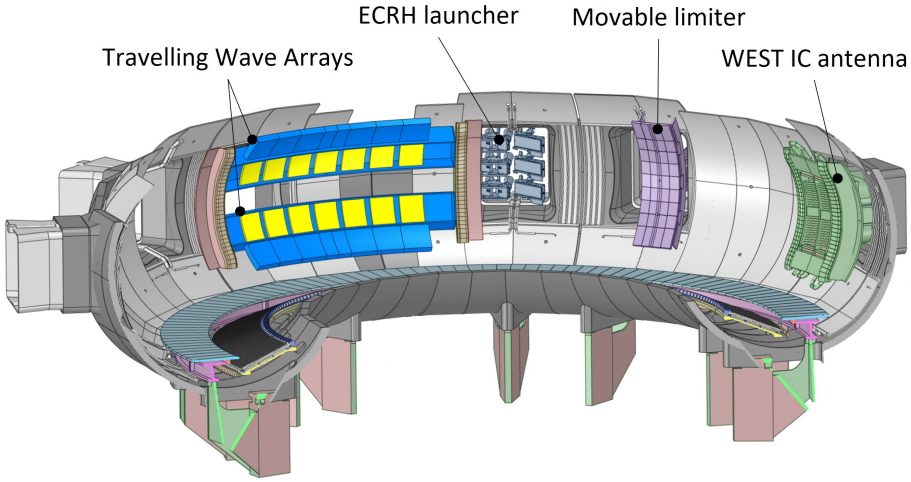

FIGURE 3. Proposed TWA antenna for WEST.

22 August 2023 18:13:25

The frequency response sensitivity of the structure was calculated by modelling the thermal-mechanical deformation of the structure [45], and creating an equivalent perturbation of the capacitor layout used in the RF modelling. This simple but effective method avoids expensive simulations, and has been experimentally verified. In particular, the maximum fields in the antenna components were calculated. The design limit was fixed at 2.5 kV/mm. Dedicated probes were designed to monitor this value during the experimental phase.

The antenna mock-up was manufactured by ASIPP and installed in the TITAN facility in CEA-Cadarache. An experimental activity demonstrated the performance of the antenna in vacuum to be compliant with the design expectation [42], both at low (up to 200 kW) and at high (up to 2 MW) power. The frequency response was monitored during thermal deformation induced by radiative load (i.e. baking of the vessel) and by RF-induced ohmic loss. The antenna showed resilience to thermo-mechanical deformations. Up to the maximum available power from the generator (2 MW) was launched into the antenna, validating the maximum fields expected on the monitored antenna components. Pulses of 500 kW lasting 60 s were repeated to test the performance of the antenna while monitoring the out-gassing from the structure and the signatures of anomalous behaviours (e.g. arcs). All the tests were successful.
Additionally, the ohmic losses of the antenna were experimentally measured and compared to the values expected by modelling. The power loss fraction remains below 4%, a positive result when considering that all the antenna components were made of stainless steel only.

PLASMA-WALL INTERACTIONS ASPECTS

One of the key features of the TWA is its larger number of radiating elements when compared to a classical in-port antenna. This allows to reduce the fields excited by the TWA for the same amount of power coupled to the plasma, by reducing the antenna power density. This characteristic should reduce the Plasma-Wall Interactions (PWIs) induced by the antenna during its operation.

On top of this intrinsic advantage, the possibility of further reducing PWIs was investigated recently. Following the experimental and numerical advances on ICRH-induced PWIs, the analysis concentrated on two criteria that appear to correlate well with enhanced PWIs: (i) the low toroidal part of the power spectrum launched by the antenna which best relates to far-field sheath and which can lead to an excitation of edge modes and edge power losses in the presence of an LH resonance in the edge plasma density profile. (ii) the near-fields taking place on the PFCs (*e.g.* limiters), which best relates to near-field sheath and ponderomotive force taking place near the antenna hardware.
In conventional ICRF antennas, those two criteria are controlled by actively varying the current distribution of the antenna straps in amplitude and phase [29]. In a TWA, the current distribution depends on the dispersion relation of the structure. This is a function of the frequency and ultimately depends on the capacitor layout used to tune the

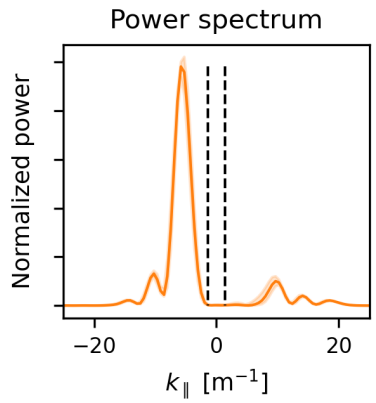

FIGURE 4. TWA antenna power spectrum minimizing the low-$|k_\parallel|$ part (dashed lines). The solid line represents the spectrum for the capacitor nominal values. The shaded area represents its sensitivity to variations of the capacitor values of $\pm$ 5%.

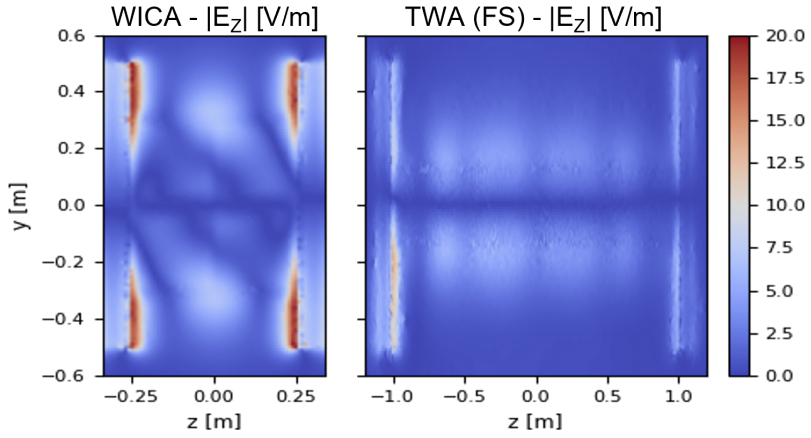

FIGURE 5. Electric field amplitude, toroidal component, (left) of the WEST antenna and (right) of the TWA antenna. The fields are calculated on a surface 3 mm in front of the limiters. The maximum values are 24 and 14 V/m for the WEST and TWA antennas, respectively.

22 August 2023 18:13:25

antenna.

Therefore, the fields and the power spectrum launched by the antenna can be tailored by varying the capacitor layout tuning each strap. The optimization took into account the low-$k_{\|}$ region, the toroidal component of the electric field E_z, and the bandwidth of the antenna. Figure 4 demonstrates the possibility to reduce the low toroidal content of the TWA power spectrum using this method. The solid line is the power spectrum for an optimized capacitor layout. The dashed lines indicate the low-$k_{\|}$ region $|k_{\|}| < k_0$.

Moreover, the stability of the optimized spectrum was evaluated by randomly varying the capacitor layout around its reference values with perturbations extracted from a uniform distribution corresponding to $\pm$ 5% of the capacitor nominal values. This capacitance error value is overestimating the capacitance deviation expected in an experiment. The result is shown by the shaded area in Fig. 4, and it is barely noticeable. The spectrum is insensitive to these variations and remains clean from low-$k_{\|}$ excitation.

Figure 5 shows the toroidal component of the electric field $|E_z|$ calculated on a surface located 3 mm in front of the antenna limiters, for a coupled power of 1 W. The top panel shows $|E_z|$ for the WEST antenna, and the bottom panel the field of the TWA. Both antennas were equipped with a Faraday shield (FS); aligned to the magnetic field for the WEST antenna, and aligned with the toroidal direction, i.e. horizontal, for the TWA. No significant difference between the parallel (to the magnetic field) and toroidal component of the electric field is observed in the calculations. The field of the WEST antenna is peaked on the four corners of the limiters. Its maximum value is 24 V/m. The TWA field is asymmetric and peaked only in the bottom left corner, with its maximum at 14 V/m. This represents a reduction of 42% compared to the WEST antenna. The two antennas were loaded with the same plasma profile, reconstructed from experimental data of the WEST shot #56898 at $t = 6$ s.

Another peculiarity of this TWA design is that the straps are recessed by 2 cm compared to the WEST antenna. In the above computations, the distance of the strap to a reference point on the profile was set equal for the two antennas, effectively moving the plasma away from the WEST antenna by 2 cm.

An extensive analysis of the capacitor layout optimization procedure and the sensitivity of the TWA antenna spectra to load, to frequency, and to capacitor layout is presented in a companion paper [47].

22 August 2023 18:13:25

A TWA RESONANT RING SYSTEM AND ITS CONTROL ASPECTS

In this section, we present a complete system composed of a TWA antenna and a feeding system based on the resonant ring configuration [6, 15, 16, 17]. In particular, we discuss the system control aspects leveraging the combined characteristics of the resonant ring and of the TWA antenna.

First, we examine the characteristics of the TWA antenna alone. The power is fed to the input port of the structure. The reflected power fraction is low when the antenna is operated inside its bandwidth. Depending on the coupling conditions, a fraction of the power is transmitted to the output port, leaving the structure. The difference between the two is the power coupled to the plasma, minus a few per cent of ohmic loss. Figure 6 shows the reflected, transmitted and coupled power fractions, as a function of frequency. The solid line represents the frequency response for the capacitor nominal value. The shaded areas represent the sensitivity of the frequency response to thermo-mechanical deformations and manufacturing tolerances. To model those uncertainties, the capacitor layout was perturbed by

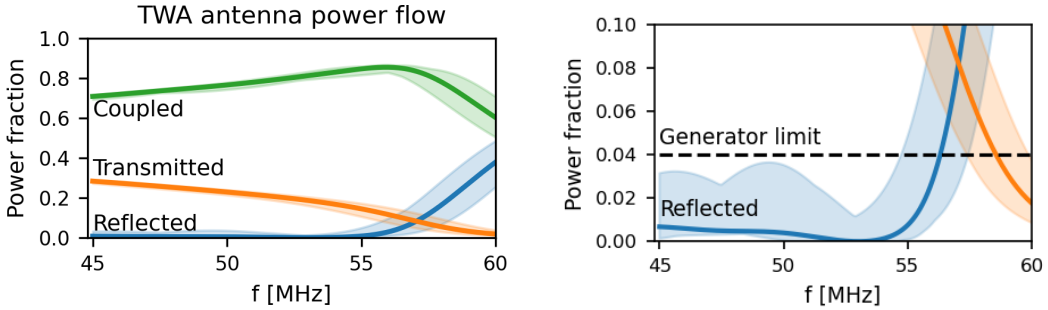

FIGURE 6. Power reflected at the input, transmitted to the output and coupled to the plasma (plus ohmic loss) as a function of frequency. The shaded areas shows the sensitivity of the response to a uniformly distributed random capacitor variation of 5% of the nominal values, represented by the solid lines. (right panel) magnification of the left panel with the generator limit highlighted.

adding a term, on each capacitor, extracted from a uniform distribution covering ±5% of the capacitor nominal values. This simple, but effective, way of taking into account those uncertainties was experimentally validated on the antenna mock-up [42].

The bottom panel of figure 6 shows a magnified portion of the top panel. The dashed line indicates the generator limit, set to VSWR 1:1.5, corresponding to 4% of reflected power. Inside the bandwidth, i.e., below 55 MHz, the antenna could be directly connected to a generator, tolerating even the large fluctuations of the tuning capacitor layout of the sensitivity analysis. The top panel of the same figure shows a coupled fraction of 70-80% and 20-30% of the power leaving the structure, effectively demonstrating the low reflection of the TWA component. This fraction could be damped in a dummy load, or recirculated back to the input of the antenna by using a resonant ring.

Figure 7 shows a sketch of a resonant ring feeding circuit connected to a TWA antenna. The main element of the ring is the variable coupler, composed of two hybrid couplers (Hyb) and a phase shifter (PS). This phase shifter could be implemented with a line stretcher (LS). The principle of operation of the ring is indicated by means of the sinusoidal signal traces. One input of the first hybrid coupler is connected to the generator. The other is connected to the TWA output port, to recirculate the uncoupled power. The phase shifter LS-TWA is used to put in phase the two input signals. The hybrid coupler is mixing the two signals on its output ports. The phase shifter LS-VC introduces a phase shift between the input ports of the second hybrid coupler, such that the signals cancel out on the dummy load branch, and sum up on the TWA input side. The main advantage of this recirculating scheme is that the coupled power (+ the ohmic losses) equals the generator power. The case sketched in figure 7 is for two input signals of equal amplitude. However, the same principle is valid for signals of different amplitudes. For a practical example, in the case of figure 6 the recirculated fraction is 25%.

Figure 8 presents the percentage of the power lost in the dummy load, as a function of the electrical length of the two phase shifters, LS-TWA and LS-VC. The three panels show the phase-space for three different conditions. The top panel shows the reference initial conditions, where the ring is tuned, i.e., the fraction of power lost in the dummy load is minimized, and the minimum is marked with a white circle. The two PS are now locked in position and the dashed red lines represent the contour of 2%. The middle panel represents the phase space after a *rigid* shift of the density profile by 1 cm away from the antenna. There is a new minimum (red marker), located in a different position compared to the current one (white circle). A controller could be used to re-tune the ring by acting on the line stretchers, bringing the white dot on top of the red one. However, a similar effect is obtained by increasing the operating frequency by 1 MHz (bottom panel), without having to act on the line stretchers. The advantage is that frequency variations are quicker than physical movements of the line stretchers. Nevertheless, the minimum does not coincide with the actual position in phase space. Only the position of LS-TWA is recovered, while LS-VC still presents a difference. However,

22 August 2023 18:13:25

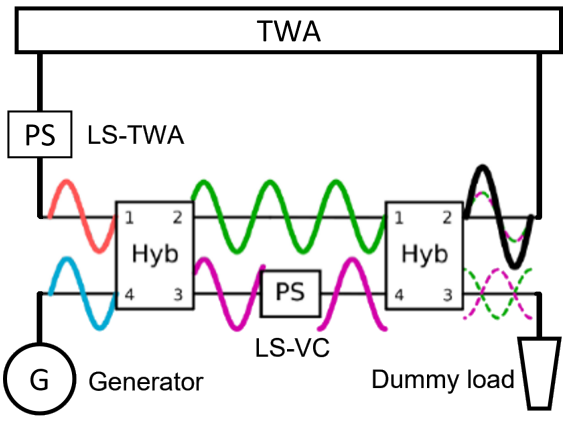

FIGURE 7. Schematic of the resonant ring. The sketched waveforms indicate the principles of operation. The two phase shifters (PS) combine the power from the generator and the one recirculated from the TWA such that the power in the dummy load is minimized.

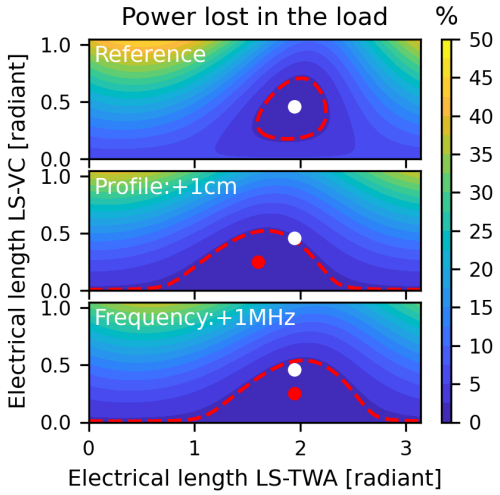

FIGURE 8. Percentage of power lost in the dummy load, as a function of the line-stretchers length. The white dot is the minimum for the reference case. The dashed red line is the 2% contour. (top) initial configuration, (middle) plasma profile moves 1 cm away from the antenna, (bottom) operating frequency increased by 1 MHz.

the current position (the white dot) is within 2%, an acceptable value. The above calculation shows that the resonant ring system has low sensitivity to plasma load variations and to frequency variations.
From another perspective, we are interested in using the frequency as an actuator to control the power deposition location, which depends on the frequency and the wavenumber. The low sensitivity of the ring to frequency variations is instrumental for this function. Indeed, it allows to maintain maximal power delivered to the antenna while sweeping the driving frequency. Moreover, the low sensitivity of the spectrum to frequency variations allows maintaining the maximum of the power spectrum around the same wavenumber. The core physics aspects and prospects are discussed in the next section.

CORE PHYSICS ASPECTS

The launched TWA power spectrum presents an enhanced directivity, when compared to a WEST ICRH antenna (WIC), enabling a more local power deposition in the plasma core [14]. Figure 9 shows the power deposition profiles calculated with EVE code [48] at two frequencies. The heating scheme was minority Hydrogen in Deuterium, D(H)[5%], with 3.47 T at 2.5 m.
At 55.5 MHz, the WIC has a broader deposition profile, while for the TWA the profile is peaked around $\rho \approx 0.3$. This is an effect of the reduced power deposition spreading due to Doppler shift caused by $k_{//}$ and finite temperature effects. For the investigated case, the narrower TWA spectrum enhances the power absorption on the high field side of the magnetic axis (see Fig.8 in [14]).
At 52.5 MHz We obtain profiles peaked on-axis for both antennas. However, the WIC deposition is broader when compared to the TWA one. The development of a dedicated scenario to investigate the core physics performance of the TWA, and compare it to the performance of the WEST antennas, will be covered in a future publication.
As discussed in the previous sections, another feature of the antenna is its large bandwidth, allowing the antenna to be passively matched for a large range of frequencies. Moreover, we have demonstrated that the antenna spectrum and the resonant ring are insensitive to frequency variations. All the above features combined open up the possibility to actively control the power deposition profile inside the plasma core by acting on the driving frequency of the power generators. This can be quickly changed within the generator bandwidth, which is 4 MHz for the WEST RF plant, resulting in an excursion of the resonant layer of ≈15 cm. Work is on-going to investigate the use of the antenna for active plasma control.

22 August 2023 18:13:25

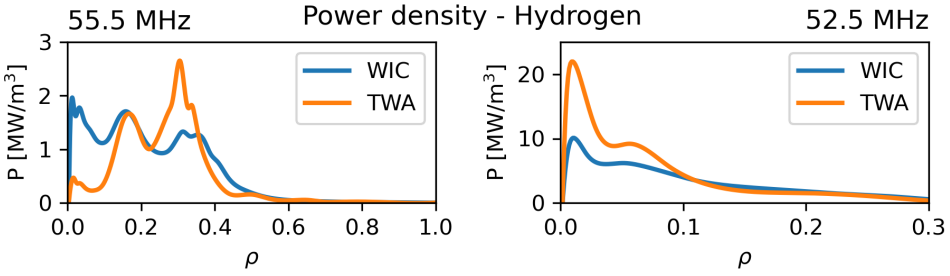

FIGURE 9. Power deposited on the minority Hydrogen for the WEST antenna (WIC) and the TWA, calculated with the EVE code. At 55.5 MHz (left panel), the TWA shows off-axis peaked absorption and the WIC a broad profile. At 52.5 MHz (right panel), both profiles are peaked on-axis, with more localized deposition for the TWA.

SUMMARY AND FUTURE PROSPECTS

In this paper, we have presented an overview of the TWA concept proposed for a future fusion reactor like EU-DEMO. It consists of several TWA sections with, many elements, to decrease the system power density (≈ 1.1 MW/m^2). We discussed the latest integration proposal for a TWA antenna as part of the breeding blanket modules, using the HCPB as a reference blanket design, showing its relatively low impact on the TBR of the reactor. The antenna will act as first wall and shares the cooling with the blanket. Further work is ongoing to define the interfaces between the TWA antenna and the feeding lines.

We then focused on the necessary steps foreseen to demonstrate the feasibility of this reactor-relevant technology on a device like WEST. We briefly discussed the proposed system, to focus on the encouraging results obtained with an experimental mock-up, which was tested in the TITAN facility at low and high power (up to 2 MW).

We presented the recent theoretical steps taken to further optimize the proposed system for WEST and DEMO. In particular, we demonstrate the possibility to optimize the power spectrum launched by the antenna. The aim is further to reduce the near-fields taking place on the PFCs near the antenna structure.

We described the most promising feeding scheme for a TWA, which is based on a resonant ring, highlighting its working principle and its features. We also acknowledge the possibility to change the power deposited in the plasma core by actively changing the antenna driving frequency.

Further work could be done to assess the sensitivity of the optimization to variations in the geometrical parameters of the antenna. Additionally, the possibility to use a non-constant strap inter distance, and/or strap width, to tailor the antenna response could open up a new optimized design, pushing the limit of the models currently used. Moreover, integrated modelling of the RF physics from the edge to the core could provide more insights into the interaction of the TWA with the plasma edge.

The possibility to develop a TWA launcher for plasma start-up and wall conditioning studies is under consideration for the NORTH [49] device. The modest power requirements (< 10 kW) allow designing a compact antenna, despite the low frequency dictated by the achievable magnetic field (< 0.3 T). The plasma parameters routinely achieved in NORTH are representative of the edge of bigger machines, i.e., $T_e \approx 10$ eV and $n_e < 10^{17}$ m^{-3}. The device could be a suitable platform to investigate the interaction of a TWA antenna with an edge plasma. It could contribute to the investigations on edge physics phenomena like sheath rectification, ponderomotive force, or LH resonance absorption, which are difficult to study in bigger devices.

ACKNOWLEDGMENTS

This work has been carried out within the framework of the EUROfusion Consortium, funded by the European Union via the Euratom Research and Training Programme (Grant Agreement No 101052200 — EUROfusion). Views and opinions expressed are however those of the author(s) only and do not necessarily reflect those of the European Union or the European Commission. Neither the European Union nor the European Commission can be held responsible for them.

The author R.R. would like to acknowledge the support from the Otto Mønsteds Fond and from VILLUM Fonden research grant 15483.

REFERENCES

1. S. C. Chiu, C. P. Moeller, V. S. Chan, and F. P. Blau, "Study of the slow-wave structure as an ICRF launcher," Nuclear Fusion **24**, 717 (1984).
2. F. Durodié, M. Vrancken, R. Bamber, L. Colas, P. Dumortier, D. Hancock, *et al.*, "Performance assessment of the iter icrf antenna," AIP Conference Proceedings **1580**, 362–365 (2014).
3. J. Ongena, A. Messiaen, Y. O. Kazakov, R. Koch, R. Ragona, V. Bobkov, *et al.*, "Recent advances in physics and technology of ion cyclotron resonance heating in view of future fusion reactors," Plasma Physics and Controlled Fusion **59**, 054002 (2017).
4. D. Van Eester, E. Lerche, R. Ragona, A. Messiaen, T. Wauters, *et al.*, "Ion cyclotron resonance heating scenarios for DEMO," Nuclear Fusion **59**, 106051 (2019).
5. A. Messiaen and R. Weynants, "Icrh antenna coupling physics and optimum plasma edge density profile. application to ITER," Plasma Physics and Controlled Fusion **53**, 085020 (2011).
6. C. P. Moeller, S. C. Chiu, and D. A. Phelps, "A combline structure for launching unidirectional fast waves," Europhys. Conf. Abs. **16E**, 5 (1992).
7. G. Matthaei, "Combline bandpass filters of narrow or moderate bandwidth," Microwave Journal **6**, 82–91 (1963).
8. K. Chang, *Encyclopedia of RF and Microwave Engineering, Volumes 1 - 6* (John Wiley & Sons, 2005) pp. 674–694.
9. A. Messiaen, M. Vervier, P. Dumortier, D. Grine, P. Lamalle, F. Durodié, *et al.*, "Preparing ITER ICRF: development and analysis of the load resilient matching systems based on antenna mock-up measurements," Nuclear Fusion **49**, 055004 (2009).
10. H. Ikezi and D. Phelps, "Traveling-wave antenna for fast-wave heating and current drive in tokamaks," Fusion technology **31**, 106–117 (1997).
11. T. Ogawa, K. Hoshino, S. Kanazawa, M. Saigusa, T. Ido, H. Kawashima, *et al.*, "Radiofrequency experiments in JFT-2M: Demonstration of innovative applications of a travelling wave antenna," Nuclear Fusion **41**, 1767–1775 (2001).
12. D. A. Phelps, C. P. Moeller, H. Ikezi, and S. C. Chiu, "First demonstration of a traveling wave antenna in a tokamak and relevance to the JFT-2M combline," AIP Conference Proceedings **355**, 380–383 (1996).
13. D. A. Phelps, F. W. Baity, R. W. Callis, J. S. deGrassie, C. P. Moeller, and R. I. Pinsker, "Advantages of traveling wave resonant antennas for fast wave heating systems," AIP Conference Proceedings **403**, 397–400 (1997).

22 August 2023 18:13:25

14. R. Ragona, A. Messiaen, J. Bernard, E. Delchambre, R. Dumont, F. Durodié, *et al.*, "Traveling wave array for demo with proof of principle on WEST," Fusion Engineering and Design **146**, 854–857 (2019).
15. R. Ragona and A. Messiaen, "Conceptual study of an ICRH traveling-wave antenna system for low-coupling conditions as expected in DEMO," Nuclear Fusion **56**, 076009 (2016).
16. F. Tischer, "Resonance properties of ring circuits," IRE Transactions on Microwave Theory and Techniques **5**, 51–56 (1957).
17. S. J. Miller, "The traveling wave resonator and high power microwave testing," Microwave Journal , 50–58 (1960).
18. Y. Takase, A. Ejiri, N. Kasuya, T. Mashiko, S. Shiraiwa, L. Tozawa, *et al.*, "Initial results from the TST-2 spherical tokamak," Nuclear Fusion **41**, 1543–1550 (2001).
19. Y. Takase, C. Moeller, T. Seki, N. Takeuchi, T. Watari, R. Callis, *et al.*, "Development of a fishbone travelling wave antenna for LHD," Nuclear Fusion **44**, 296–302 (2004).
20. J. Jo, J. Wang, H. Lee, S. Kim, B. Lee, S. Kim, and Y. Hwang, "Coupling study of fast wave near the lower hybrid frequency range in VEST," Physics of Plasmas **25**, 082511 (2018).
21. Y. Takase, A. Ejiri, T. Inada, C. Moeller, T. Shinya, N. Tsujii, *et al.*, "Plasma current start-up using the lower hybrid wave on the TST-2 spherical tokamak," in *AIP Conference Proceedings*, Vol. 1689 (2015) p. 080013.
22. R. Pinsker, R. Prater, C. Moeller, J. deGrassie, C. Petty, M. Porkolab, *et al.*, "Experiments on helicons in DIII-D investigation of the physics of a reactor-relevant non-inductive current drive technology," Nuclear Fusion **58**, 106007 (2018).
23. J. F. Tooker, A. Nagy, J. deGrassie, C. Moeller, M. Hansink, B. Fishler, *et al.*, "Development of a high power Helicon system for DIII-D," **123**, 228–231 (2017).
24. H. Wi, S. Wang, H. Kim, and J. Kwak, "Design and rf test of a prototype traveling wave antenna for helicon current drive in KSTAR," Fusion Engineering and Design **126**, 67–72 (2018).
25. Y. Takase, T. Wakatsuki, A. Ejiri, H. Kakuda, C. P. Moeller, T. Ambo, *et al.*, "Plasma Curent Start-up Experiment using Waves in the Lower Hybrid Frequency Range in TST-2," AIP Conference Proceedings **1406**, 427–430 (2011).
26. R. Ragona, A. Messiaen, J. Ongena, D. V. Eester, M. V. Schoor, J.-M. Bernard, J. Hillairet, and J.-M. Noterdaeme, "A travelling wave array system as solution for the ion cyclotron resonance frequencies heating of DEMO," Nuclear Fusion **60**, 016027 (2019).
27. L. Colas, G. Urbanczyk, M. Goniche, J. Hillairet, J.-M. Bernard, C. Bourdelle, *et al.*, "The geometry of ICRF – induced wave-SOL interaction.a multi-machine experimental review in view of ITER operation." Nuclear Fusion (2021).
28. V. Bobkov, D. Aguiam, R. Bilato, S. Brezinsek, L. Colas, A. Czarnecka, *et al.*, "Impact of ICRF on the scrape-off layer and on plasma wall interactions: From present experiments to fusion reactor," Nuclear Materials and Energy **18**, 131–140 (2019).
29. V. Bobkov, F. Braun, R. Dux, A. Herrmann, H. Faugel, H. Fünfgelder, *et al.*, "First results with 3-strap ICRF antennas in ASDEX upgrade," Nuclear Fusion **56**, 084001 (2016).
30. Y. Lin, J. C. Wright, and S. J. Wukitch, "Physics basis for the ICRF system of the SPARC tokamak," Journal of Plasma Physics **86**, 865860506 (2020).
31. D. Van Eester and K. Crombé, "A crude model to study radio frequency induced density modification close to launchers," Physics of Plasmas **22**, 122505 (2015).
32. H. Kohno, J. Myra, and D. D'Ippolito, "Numerical investigation of fast-wave propagation and radio-frequency sheath interaction with a shaped tokamak wall," Physics of Plasmas **22**, 072504 (2015).
33. V. Maquet and A. Messiaen, "Optimized phasing conditions to avoid edge mode excitation by ICRH antennas," Journal of Plasma Physics **86**, 855860601 (2020).
34. A. Messiaen and V. Maquet, "Coaxial and surface mode excitation by an ICRF antenna in large machines like DEMO and ITER," Nuclear Fusion **60**, 076014 (2020).
35. A. Messiaen, V. Maquet, and J. Ongena, "Ion cyclotron resonance heating fast and slow wave excitation and power deposition in edge plasmas with application to ITER," Plasma Physics and Controlled Fusion **63**, 045021 (2021).
36. V. Maquet, A. Druart, and A. Messiaen, "Analytical edge power loss at the lower hybrid resonance: Antiter iv validation and application to ion cyclotron resonance heating systems," Journal of Plasma Physics **87**, 905870617 (2021).
37. J. M. Noterdaeme, A. Messiaen, R. Ragona, W. Zhang, A. Bader, F. Durodié, *et al.*, "Progress on an ion cyclotron range of frequency system for DEMO," Fusion Engineering and Design **146**, 1321–1324 (2019).
38. V. Bobkov, M. Usoltceva, H. Faugel, A. Kostic, R. Maggiora, D. Milanesio, *et al.*, "Development of pre-conceptual ITER-type ICRF antenna design for DEMO," Nuclear Fusion **61**, 046039 (2021).
39. M. Usoltceva, V. Bobkov, H. Faugel, T. Franke, A. Kostic, R. Maggiora, *et al.*, "DEMO ion cyclotron heating: Status of ITER-type antenna design," Fusion Engineering and Design **165**, 112269 (2021).
40. A. Messiaen and R. Ragona, "Modeling of the Traveling Wave Antenna in view of the ICRF heating of DEMO," EPJ Web of Conferences **157**, 03033 (2017).
41. R. Ragona and A. Messiaen, "Study of a distributed ICRF antenna system in DEMO," EPJ Web of Conferences **157**, 03044 (2017).
42. R. Ragona, F. Durodié, A. Messiaen, J. Ongena, M. V. Schoor, S. Agzaf, *et al.*, "Status of the WEST travelling wave array antenna design and results from the high power mock-up," Nuclear Fusion **62**, 026046 (2022).
43. F. A. Hernández, P. Pereslavtsev, G. Zhou, H. Neuberger, J. Rey, Q. Kang, *et al.*, "An enhanced, near-term HCPB design as driver blanket for the EU DEMO," Fusion Engineering and Design **146**, 1186–1191 (2019).
44. A. Bader *et al.*, "Integration scenario of a travelling wave antenna in european demo," (2022), unpublished.
45. T. Batal, R. Ragona, J. Hillairet, C. Yu, J.-M. Bernard, P. Mollard, *et al.*, "Design and thermal-structural analysis of a high power ICRH travelling wave array antennas," Fusion Engineering and Design **166**, 112325 (2021).
46. R. Ragona, J. Hillairet, F. Durodié, C. Yu, P. Mollard, Q. Yang, *et al.*, "RF network analysis of the WEST TWA mock-up in TITAN," Fusion Engineering and Design **168**, 112615 (2021).
47. V. Maquet, R. Ragona, F. Durodié, and J. Hillairet, "Minimization of the edge modes and near fields of a travelling wave array antenna for WEST," (2022), submitted to Nuclear Fusion.
48. R. J. Dumont, "Variational approach to radiofrequency waves in magnetic fusion devices," Nuclear Fusion **49**, 075033 (2009).
49. S. K. Nielsen, M. P. Gryaznevich, A. S. Jacobsen, T. Jensen, M. Jessen, S. B. Korsholm, *et al.*, "First results from the NORTH tokamak," Fusion Engineering and Design **166**, 112288 (2021).

22 August 2023 18:13:25